Acta Cryst. (1998). D**54**, 1008–1011

Crystallization and preliminary X-ray crystallographic studies of the 13-fold symmetric portal protein of bacteriophage SPP1

PETRA JEKOW,[a,b] SIGRID SCHAPER,[b] DIRK GÜNTHER,[b]† PAULO TAVARES[b]‡ AND WINFRIED HINRICHS[a]* *at* [a]*Freie Universität Berlin, Institut für Kristallographie, Takustrasse 6, D-14195 Berlin, Germany, and* [b]*Max Planck Institut für Molekulare Genetik, Ihnestrasse 73, D-14195 Berlin, Germany. E-mail: winfried@chemie.fu-berlin.de*

(*Received 5 January 1998; accepted 11 February 1998*)

Abstract

Portal proteins are cyclical oligomers which play essential roles in bacteriophage pro-capsid formation, DNA packaging, and in connector formation. Bacteriophage SPP1 portal protein (gp6) is a turbine-like molecule with 13-fold symmetry [Dube *et al.* (1993) *EMBO J.* **12**, 1303–1309]. The purified protein was crystallized with polyethylene glycol 400 as the precipitating agent using the vapor-diffusion method. Salt conditions were selected based on the properties of gp6 in different ionic environments. X-ray diffraction data up to a resolution of 7.85 Å were measured from frozen crystals with orthorhombic space group $C222_1$ and cell dimensions a = 180.5 (5), b = 223.5 (5), c = 417 (1) Å. The asymmetric unit contains one tridecameric portal protein with 57.3 kDa subunits. The self-rotation searches confirm the 13-fold symmetry of the crystallized protein.

1. Introduction

Portal proteins are ubiquitous among tailed bacteriophages that encapsidate double-stranded DNA. These cyclical homo-oligomers are located at a single vertex of the icosahedral viral capsid that binds to the tail (for reviews see Valpuesta & Carrascosa, 1994; Casjens & Hendrix, 1988). They are essential for assembly of the functional pro-capsid, for DNA packaging, and serve as the docking site for the phage tail (Valpuesta & Carrascosa, 1994). These roles are accomplished by a sequential program of protein–protein and putative protein–DNA interactions occurring during viral morphogenesis. The multifunctional properties of portal proteins make them most interesting assemblies for studying the molecular mechanisms underlying such type of interactions.

Bacteriophage SPP1 portal protein (gp6) is encoded by gene *6* of the phage genome (Tavares *et al.*, 1992). The protein is composed by 13 identical subunits of 57.3 kDa (Jekow *et al.*, 1998). Its structure was solved at 18 Å resolution by cryo-electron microscopy and single-particle image-processing techniques showing a turbine-like molecule with a central channel which spans its full height (Tavares *et al.*, 1995). Gp6 is formed by a conical stem that holds the structure together, 13 well individualized wings that irridiate up and outwards from the stem, and an internal less defined domain that surrounds the top region of the central channel at the height of the wings. The latter region is apparently flexible and might differ somehow between the gp6 wild type and SizA (Orlova *et al.*, 1998). Gp6 SizA carries a single amino-acid substitution ($Asn_{365} \rightarrow Lys$) that is responsible for the packaging of reduced amounts of DNA during bacteriophage SPP1 morphogenesis (Tavares *et al.*, 1992).

The gp6 cyclical molecule is assembled by addition of monomers to a growing curvilinear oligomer that closes into a metastable circular ring with 13 subunits (Van Heel *et al.*, 1996). The number of protomers in the structure is thus defined by the angle between adjacent subunits and also by the increased bending imposed by closure of the ring (Van Heel *et al.*, 1996). These features vary between portal proteins from different phage origin as 12-fold symmetric assemblies (T4: Driedonks *et al.*, 1981; lambda: Kochan *et al.*, 1984; T3: Carazo *et al.*, 1986; P22: Bazinet *et al.*, 1988) and polymorphisms of 12- and 13-mers (φ29: Dube *et al.*, 1993; Valpuesta *et al.*, 1994; Tsuprun *et al.*, 1994; T7: Kocsis *et al.*, 1995) have also been described.

In order to understand the molecular basis of gp6 multi-functionality during phage morphogenesis and the organization of the 13-mer we aim to combine structural information from high-resolution X-ray crystallography with genetic, functional and biochemical data. Here we report the crystallization of the 745 kDa cyclical oligomer gp6 and initial crystallographic studies.

2. Material and methods

2.1. *Gp6 overproduction and purification*

Gp6 (wild type or SizA) was overproduced from *Escherichia coli* BL21 (DE3) (pLysS) bearing a chimeric pBluescript SK(+) plasmid carrying the selected gene *6* allele (Jekow *et al.*, 1998). After harvesting and lysis of the cells, the protein was purified by ammonium sulfate precipitation and anion-exchange chromatography as described (Jekow *et al.*, 1998). In the last purification step on a size-exclusion chromatography column (Superose 6, Pharmacia), the salt conditions in the buffer (20 m*M* Hepes/NaOH pH 7.6) were changed from 500 m*M* NaCl to 5 m*M* $MgCl_2$ by first rebuffering the protein sample in Centrex microconcentrators (cutoff 100 kDa, Schleicher & Schuell) and subsequent running on the column with the appropriate buffer. The protein peak eluting from the column was fractionated in three parts: the ascending, the middle and the descending part of the peak. Only the middle and descending part of the peak were concentrated in Centrex microconcentrators to 10 mg ml^{-1} protein for crystallization assays. The protein concentration was determined spectroscopically using the absorption coefficient of 802 875 M^{-1} cm^{-1} at 280 nm as determined experimentally for the 745 kDa tridecameric protein (Günther, 1994).

† Present address: Max Planck Institut für Infektionsbiologie, Monbijoustrasse 2, D-10117 Berlin, Germany.

‡ Present address: Unité de Pathogénie Microbienne Moléculaire et Unité INSERM 389, Institut Pasteur, 28 Rue du Docteur Roux, 75724 Paris CEDEX 15, France.

© 1998 International Union of Crystallography
Printed in Great Britain – all rights reserved

ISSN 0907-4449 © 1998

Table 1. *Data collection statistics*

Data set	Gp6 SizA	
Space group	$C222_1$	
Cell dimensions at 100 K		
a (Å)	180.5 (5)	
b (Å)	223.5 (5)	
c (Å)	417 (1)	
Wavelength (Å)	0.9996	
Resolution range (Å)	80.0–7.85	
Number of measured reflections	42742	
Number of unique reflections	9072	
	All data	8.10–7.85 Å resolution shell
Completeness (%)	93	86
R_{sym} (%)†	8.1	29.7
Ratio $\langle I/\sigma(I)\rangle$	17.6	3.6
Redundancy‡	4.8	4.7

† $R_{sym} = \sum_i \sum_{hkl} |I_{i,hkl} - \langle I_{hkl}\rangle| / \sum_i \sum_{hkl} \langle I_{hkl}\rangle$, where $I_{i,hkl}$ is the intensity of symmetry-redundant reflections and I_{hkl} is the mean intensity. ‡ Redundancy = number of observations/number of unique reflections.

2.2. *Crystallization*

The protein was crystallized using the hanging-drop vapor-diffusion method (McPherson, 1982). The gp6 protein solution (10 mg ml^{-1}) was buffered with 20 m*M* Hepes/NaOH, pH 7.6 and 5 m*M* $MgCl_2$. Drops containing 3 µl gp6 solution and 3 µl precipitant buffer were equilibrated against 700 µl precipitant buffer. The precipitant buffer contained 50 m*M* Hepes/NaOH pH 7.6, 100 m*M* $CaCl_2$, 10%(*v*/*v*) glycerol, 0.02%(*w*/*v*) NaN_3 and 15%(*v*/*v*) PEG 400 as the precipitating agent. Crystallization was achieved within 9 months at room temperature.

2.3. *X-ray diffraction*

A complete native data set to a resolution of 7.85 Å was measured under cryo conditions at 100 K on a Mar Research image-plate detector with a radius of 90 mm at the EMBL beamline BW7A (DORIS storage ring at DESY, Hamburg) at a wavelength of 1.0 Å. The crystallization conditions allowed flash freezing of the crystal in a gaseous nitrogen stream (Oxford Cryosystems Cryostream) without further modifications of the mother liquor concerning additional cryo protectants. 120 images were collected from one single crystal with an oscillation range of 1° and an exposure time of about 15 min per image. No significant radiation damage was observed during the whole period of data collection. The imaging-plate diffraction data were indexed and processed using the *HKL* suite of programs (Otwinowski & Minor, 1997). Details of data collection and processing are summarized in Table 1.

Self-rotation searches to identify the local symmetry of the portal protein molecule were performed with the program systems *AMoRe* (Navaza & Saludjian, 1997), *GLRF* (Tong & Rossmann, 1997), and *POLARRFN* of the *CCP*4 suite (Collaborative Computational Project, Number 4, 1994), respectively. The searches were successful within an integration radius (*r*) of 80 Å and data in the resolution shell from 7.85 to 77.0 Å in case of *AMoRe*, with $r = 84$ Å in the shell from 7.85 to 77.0 Å in case of *GLRF*, and $r = 45$ Å in the shell from 7.85 to 20.0 Å in case of *POLARRFN*.

3. Results and discussion

The best diffracting crystals were obtained with gp6 SizA. The mutant protein carries a single missense mutation (Tavares *et al.*, 1992). Comparison between SizA and the wild-type gp6 hinted at some structural differences in a top internal domain that surrounds the oligomer central channel (Orlova *et al.*, 1998). The flexibility of this region, however, did not allow a clear correlation between the mutation and a specific conformational alteration that could potentially facilitate crystallization.

Initial gp6 crystallization assays were performed with the protein in 20 m*M* Hepes/NaOH, pH 7.6 and 500 m*M* NaCl using the sparse-matrix screening method (Jancarik & Kim, 1991) in order to find crystallization conditions worth further optimization. These first crystals grew to 0.1 × 0.1 × 0.02 mm but diffracted X-rays only up to a maximum resolution of 20 Å. In the meantime, parallel work demonstrated that the ionic environment plays a significant role in gp6 structure and state of oligomerization. It was found that $MgCl_2$ in millimolar concentrations stabilizes and compacts the gp6 13-mer (Jekow *et al.*, 1998). This effect obtained with physiological concentrations of Mg^{2+} is only partly mimicked by high NaCl concentrations (*e.g.* 500 m*M*; Jekow *et al.*, 1998). gp6 solutions with Mg^{2+} were used thereafter for crystallization and a considerable improvement in crystal quality was observed.

The best crystals were obtained with gp6 in the presence of 5 m*M* $MgCl_2$. Further improvement was achieved when gp6 was fractionated on a size-exclusion column (Superose 6) and only the middle and descending part of the 13-mer elution peak were concentrated and used for crystallization. It is interesting to note that the Mg^{2+} concentration used in the chromatography experiment (5 m*M*) is at the lower border of Mg^{2+} concentrations that stabilize the protein in its 13-meric compact state (Jekow *et al.*, 1998). We suppose that a mixed population of 13-mer conformers eluted from the column and

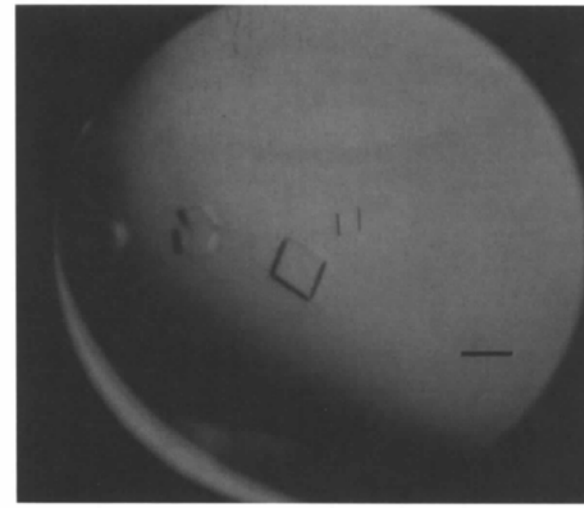

Fig. 1. Crystals of gp6 SizA grown with 15%(*v*/*v*) PEG 400 as the precipitating agent in a solution containing 50 m*M* Hepes/NaOH pH 7.6, 100 m*M* $CaCl_2$, 10%(*v*/*v*) glycerol, and 0.02%(*w*/*v*) NaN_3. The gp6 protein solution (10 mg ml^{-1}) was buffered with 20 m*M* Hepes/NaOH, pH 7.6 and 5 m*M* $MgCl_2$. The crystallization assays were performed using the hanging-drop vapour-diffusion method. The bar represents 0.2 mm.

that the more compact molecules elute with the second part of the protein sample. This compact state of the protein might facilitate its crystallization. Increased $MgCl_2$ concentrations in the protein buffer on the other hand led to faster growing crystals with roundish edges and weak diffraction.

Optimal crystallization conditions were found using PEG 400 [15%(*v*/*v*)] as the precipitating agent (Fig. 1). $CaCl_2$ in concentrations in the millimolar range was shown to induce aggregation of gp6 (Jekow *et al.*, 1998). Its presence in the precipitating solution (100 m*M*), however, promotes crystallization probably by favouring association of the protein

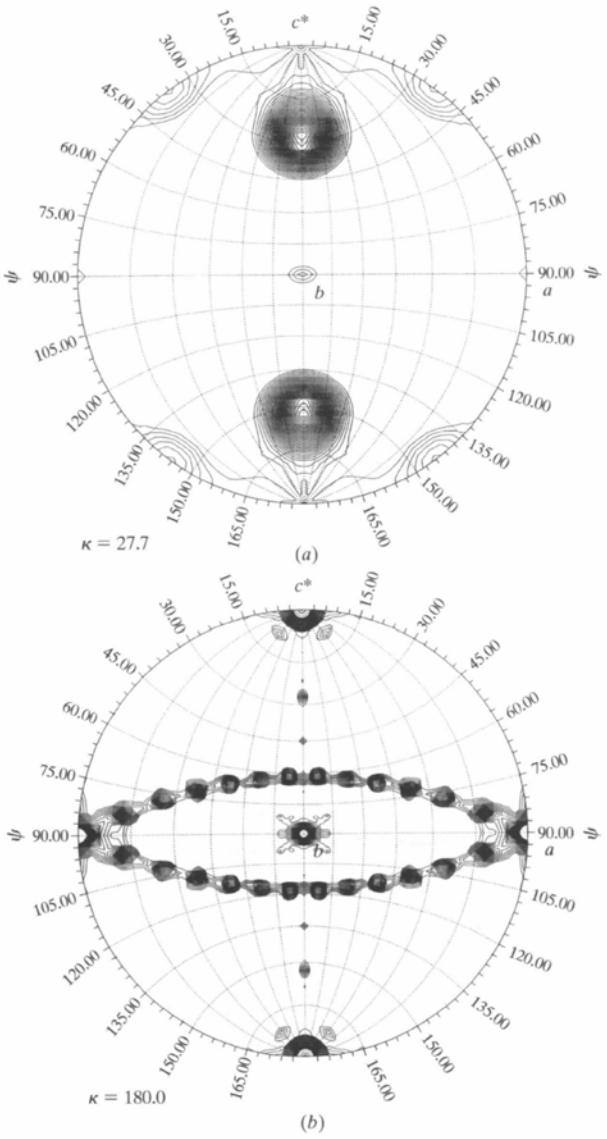

Fig. 2. Self-rotation function of gp6 mutant SizA calculated using *GLRF* (Tong & Rossmann, 1997). The stereographic projection of κ sections show φ as the radial coordinate, while ψ is given as the angular coordinate. Contour lines are drawn starting at 1σ/r.m.s. of the mean density with intervals of 0.25σ. (*a*) Section of $\kappa = 27.7^\circ \simeq 360^\circ/13$. The highest peak is located at $\varphi = 90^\circ$ and $\psi = 27.5^\circ$ identifying the orientation of the molecular axis of gp6. (*b*) Section of $\kappa = 180^\circ$. Perpendicular to the 13-fold axis ($\varphi = 90^\circ$ and $\psi = 27.5^\circ$) are 13 twofold axes resulting from the relationship of the crystallographic twofold axis (the *a* axis) and the C_{13} symmetry axis of the gp6 SizA.

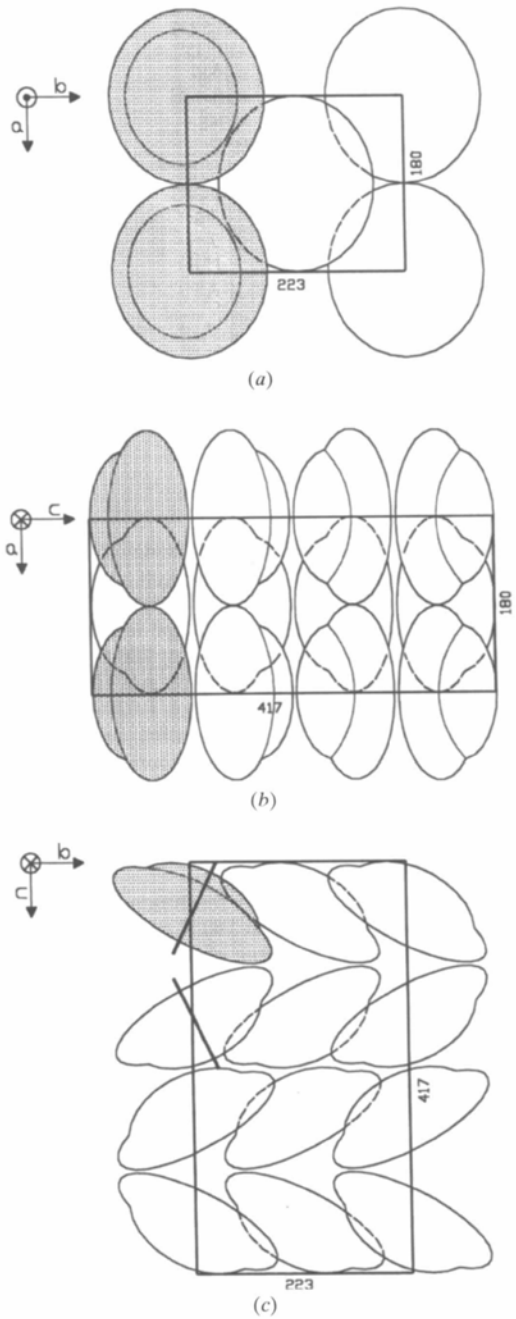

Fig. 3. Packing model for the gp6 molecules in the crystal considering the derived unit-cell parameters and the orientation of the 13-fold symmetry axis of the individual molecule. The unit-cell projection is presented by a rectangle with dimensions indicated in Å. The gp6 13-mer rough shape is based on the structure of the molecule determined by electron microscopy (Dube *et al.*, 1993). (*a*) View onto the **a,b** plane, down the *c* axis; (*b*) view onto the **a,c** plane, along the *b* axis; and (*c*) view onto the **b,c** plane, along the *a* axis. The local 13-fold symmetry axis is indicated by bold lines.

molecules for crystal packing. 10%(*v*/*v*) glycerol was added to the reservoir solution to lower the diffusion velocity, and to serve as cryo-protectant for flash freezing of the crystals for data collection at 100 K.

The parallelepiped-shaped crystals reached a size of 0.1 × 0.1 × 0.2 mm and showed a clear diffraction pattern to about 7 Å resolution. As the observed resolution limit is not a sharp cutoff, the maximum resolution is expected to be enhanced with further crystal growth and use of highly brilliant X-ray sources. This is in agreement with the quality of the first native data set (Table 1) measured under cryo-conditions at the EMBL synchrotron beamline BW7A (DESY in Hamburg, Germany).

The gp6 SizA protein crystals belong to the *C*-centered orthorhombic space group $C222_1$ with cell dimensions a = 180.5 (5), b = 223.5 (5), c = 417 (1) Å at 100 K. From about 50 systematically extinct reflections (00*l*) with odd indices l the twofold screw axis was clearly assigned. Compared to diffraction patterns measured at room temperature [cell dimensions were a = 182.9 (6), b = 224.2 (5), c = 423 (1) Å] the volume of the unit cell decreased slightly in the cold nitrogen stream. The crystal symmetry, however, remained unchanged. One tridecameric gp6 is present in the asymmetric unit with a volume per weight (V_m) of 2.8 Å^3 Da^{-1}, equivalent to a solvent content of 56.2% in the crystal (according to Matthews, 1968).

Considering the 12- or 13-fold symmetries proposed for different portal proteins, we calculated self-rotation functions using programs *AMoRe* (Navaza & Saludjian, 1997), *GLRF* (Tong & Rossmann, 1997) and *POLARRFN* (Collaborative Computational Project, Number 4, 1994) to verify and localize the local symmetry of the portal protein from SPP1. These self-rotation searches clearly confirmed the C_{13} point symmetry of the crystallized gp6 SizA. The 13-fold symmetry was identified by strong peaks in κ-sections $n360°/13$ with n = 1 to 6. The section for $\kappa = 27.7° \simeq 360°/13$ is shown in Fig. 2(*a*). The 13-fold axis is located in the **b,c** plane with an inclination angle to the c axis of $\psi = 27.5°$. The fact that the 13-fold symmetry axis is in perpendicular position ($\varphi = 90°$) to one of the crystallographic dyads (the a axis) creates an intermolecular symmetry ('packing symmetry', Klug, 1972) which can be found in the $\kappa = 180°$ section of the self-rotation search (Fig. 2*b*).

The orientation of the 13-fold axis perpendicular to a requires that the gp6 diameter is not larger than the length of a (180 Å), *i.e.* it has to be smaller in the crystal than the 205 Å found for gp6 in the three-dimensional reconstruction based on electron-microscopy data (Orlova *et al.*, 1998). We attribute this variation to the different salt conditions used for crystallization (presence of divalent cations) and for electron microscopy (only monovalent cations; Dube *et al.*, 1993). Correspondingly, hydrodynamic measurements under the two different solvent conditions showed an increase of *ca* 20% in gp6 Stokes radius when $MgCl_2$ was not present (Jekow *et al.*, 1998). A packing model for the crystallized gp6 molecules in the crystal unit cell is given in Fig. 3.

A heavy-atom derivative search is presently being carried out. In addition, attempts to solve the structure by the molecular-replacement method using the 18 Å resolution model derived from the electron microscopic data (Orlova *et al.*, 1998) and subsequent phase extension are under way. The 13-fold symmetry found in the asymmetric unit will probably facilitate improvement of phases.

Preliminary X-ray data were collected at the BW6 beamline of the MPG-ASMB at DESY, Hamburg. W. Saenger and T. A. Trautner are thanked for their continuous interest and support to the project; we also thank them and N. Krauss for critically reading the manuscript. E. V. Orlova, P. Dube and M. van Heel we thank for the courtesy of their unpublished results. PJ was partly supported by a grant of the Deutsche Forschungsgemeinschaft to WH and T. A. Trautner (Hi 617/1–1). SS was supported by grant SFB344/B6 of the Deutsche Forschungsgemeinschaft. PT was partly supported by the European Union Contract ERBBIOTCL923104.

References

Bazinet, C., Benbasat, J., King, J., Carazo, J. M. & Carrascosa, J. L. (1988). *Biochemistry* **27**, 1849–1856.
Carazo, J. M., Fujisawa, H., Nakasu, S. & Carrascosa, J. L. (1986). *J. Ultrastruct. Res.* **94**, 195–113.
Casjens, S. & Hendrix, R. (1988). *The Bacteriophages*, edited by R. Calendar, Vol. 1, pp. 15–91. New York: Plenum Press.
Collaborative Computational Project, Number 4 (1994). *Acta Cryst.* D**50**, 760–763.
Driedonks, R. A., Engel, A., ten Heggeler, B. & van Driel, R. (1981). *J. Mol. Biol.* **152**, 641–662.
Dube, P., Tavares, P., Lurz, R. & Van Heel, M. (1993). *EMBO J.* **12**, 1303–1309.
Günther, D. (1994). Diploma thesis, Freie Universität Berlin, Germany.
Jancarik, K. & Kim, S.-H. (1991). *J. Appl. Cryst.* **24**, 409–411.
Jekow, P., Behlke, J., Lurz, R., Tichelaar, W., Regalla, M., Hinrichs, W. & Tavares, P. (1998). Submitted.
Klug, A. (1972). *Cold Spring Harbor Symp. Quant. Biol.* **36**, 483–487.
Kochan, J., Carrascosa, J. L. & Murialdo, H. (1984). *J. Mol. Biol.* **174**, 433–447.
Kocsis, E., Cerritelli, M. E., Trus, B. L., Cheng, N. & Steven, A. C. (1995). *Ultramicroscopy*, **60**, 219–228.
McPherson, A. (1982). *The Preparation and Analysis of Protein Crystals*. New York: John Wiley.
Matthews, B. W. (1968). *J. Mol. Biol.* **33**, 491–497.
Navaza, J. & Saludjian, P. (1997). *Methods Enzymol.* **276**, 581–593.
Orlova, E. V., Dube, P., Beckmann, E., Zemlin, F., Lurz, R., Trautner, T. A., Tavares, P. & Van Heel, M. (1998). Unpublished work.
Otwinowski, Z. & Minor, W. (1997). *Methods Enzymol.* **276**, 307–326.
Tavares, P., Dröge, A., Lurz, R., Graeber, J., Orlova, E., Dube, P. & Van Heel, M. (1995). *FEMS Microbiol. Rev.* **17**, 47–56.
Tavares, P., Santos, M. A., Lurz, R., Morelli, G., Lencastre, H. L. & Trautner, T. A. (1992). *J. Mol. Biol.* **225**, 81–92.
Tong, L. & Rossmann, M. G. (1997). *Methods Enzymol.* **276**, 594–611.
Tsuprun, V., Anderson, D. & Egelman, E. H. (1994). *Biophys. J.* **66**, 2139–2150.
Valpuesta, J. M. & Carrascosa, J. L. (1994). *Quart. Rev. Biophys.* **27**, 107–155.
Valpuesta, J. M., Carrascosa, J. L. & Henderson, R. (1994). *J. Mol. Biol.* **240**, 281–287.
Van Heel, M., Orlova, E. V., Dube, P. & Tavares, P. (1996). *EMBO J.* **15**, 18, 4785–4788.